Paper 23 - Recent developments in the application of shallow water ship hydrodynamics in inland waterway design

Linke T.; Rauscher D.; Söhngen B.

Bundesanstalt für Wasserbau (BAW; Federal Waterways Research Institute), Karlsruhe, Germany

Email (1st author): tobias.linke@baw.de

ABSTRACT:

In waterway design problems it is often necessary to evaluate large numbers of driving situations for different boundary conditions and multiple vessel types. These computations can be effectively performed using fast-time simulators for ship movements in shallow and confined waters. For this purpose the Federal Waterways Engineering and Research Institute (BAW) develops the fast-time simulation software 'FaRAO' (German: Fahrdynamische RoutenAnalyse und -Optimierung). In this paper we present the mathematical model, the software framework and a course-following pilot based on an optimal control approach. As numerical validation a convergence analysis and two benchmark problems – a lateral offset maneuver and a ship passing a cross flow – are presented.

1 INTRODUCTION

Changing boundary conditions in inland waterway transport demand for an optimized use of existing waterway infrastructure. Examples for such changes in boundary conditions are the more extensive usage of existing waterways by generally larger and deeper draught vessels – as on the German Neckar River, which is currently being adapted to be navigable for 135m large vessels (before: 105m max. ship length), staying in general with the same fairway width (Söhngen 2015) - or the planned restrictions concerning fuel consumption and pollutant emissions by the European Union. This and the general trend to consider the possibility of self-driving vessels generate a demand for the development of fast-time simulation software for ship behavior in shallow and confined water which is fitted for optimization purposes. The aims of such an optimization could be e.g. minimizing fuel consumption with respect to aimed arrival times, the minimization of loads on river bed and banks to save maintenance costs, the reduction of pollutant emissions and the increase of the capacity utilization for existing waterway infrastructure.

The validity of such a fast-time simulator is limited by the quality of the mathematical model it is based on. Besides the basic momentum equations, several effects have to be taken into account that can be neglected for ships in open water, e.g. the varying flow velocity and depth along the ship length and the resulting hull forces or ship-ship-interaction.

This paper introduces the fast-time simulation program 'FaRAO' (German: Fahrdynamische RoutenAnalyse und -Optimierung) developed within the Hydraulic Engineering Department at the Federal Waterways Engineering and Research Institute (BAW, German: Bundesanstalt für Wasserbau). The focus will be on two aspects: The shallow water ship hydrodynamic system has been further refined and validated with physical models and real life measurements. The resulting ordinary differential equation (ODE) model can be solved by standard numerical integration methods. This dynamic model will be presented in detail. Secondly, a new software design based on modular blocks has been introduced. Besides better code maintainability, it enables the use of the fast-time simulation program with optimization algorithms to find optimal ship controls in terms of fuel consumption, safety concerns and arrival time.

To be able to apply optimization algorithms it was necessary to reduce the computational times significantly below real time. The resulting software framework will be documented and numerical results will be presented for two maneuver situations.

2 NUMERICAL MODEL

In this section we describe the numerical model on which the fast-time simulator FaRAO is based on. The declared aim of FaRAO is to deliver a computationally inexpensive, robust approximation of ship movements on a waterway with varying bathymetry and a nontrivial flowfield. While ship simulators consider the 3-dimensional movement of the ship in more detail, the fast-time simulator applies a simplified model but still yields an accurate representation ('80% solution') of the 2-dimensional ship movement. The substantially lower computational costs of the numerical time integration allow for the application to waterway design problems, where great numbers of ship trajectories have to be calculated, as well as the numerical solution of optimal control problems such as calculating energy efficient and time optimal ship paths as well minimizing the necessary the navigational space. After this design step the results of the fast-time simulator can be validated using a full frame ship simulator.

2.1 *Input Data*

For the simulation of the ship movement in the waterway, we need a model of the waterway in terms of fluid velocities and underwater topology as well as a parameterized model of the ship.

The BAW uses physical and numerical models to simulate the fluid behaviour in waterways for the evaluation of short- and long-term morphological developments. For this reason the BAW maintains two dimensional hydrodynamic-numerical (2D-HN) models delivering high-resolution vector fields for a broad range of water levels and discharge (cf. Figure 1). The resulting fluid velocities and bathymetry data is used as input for the fast-time simulator FaRAO. In order to handle the datasets

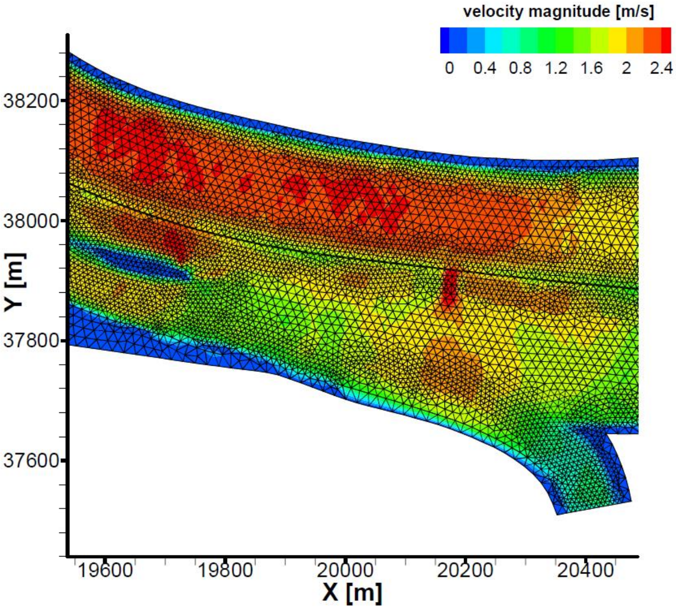

Figure 1: CFD simulation for the German river Rhine at 530 km.

for large waterway sections – the numerical mesh can easily consist of millions of grid cells – the mesh is seperated and interpolated on several smaller units ('flowfields') with rectangular, equidistant grids which are calculated in pre-processing. The computational costs for the evaluation of the flow field at a given point during runtime is substantially reduced compared to interpolation on the original numerical grid.

For the ship model, CAD data can be used to generate a segmented model consisting of cross sections representing the geometry of the ship (cf. Figure 2). Geometric values such as volume, center of mass and the hydrodynamic added masses are automatically calculated. Additional calibration parameters are determined by comparison with experimental data and/or results of 3-dimensional CFD-simulations.

To keep the number of calibration parameters as small as possible, the fast-time simulator FaRAO incorporates as much analytical and semi-empirical solutions as possible. This enables the estimation of parameters on the basis of similar ship types and is a crucial design differences in comparison to the Abkovitz model. Nevertheless, the implementation of a new ship always requires a calibration procedure.

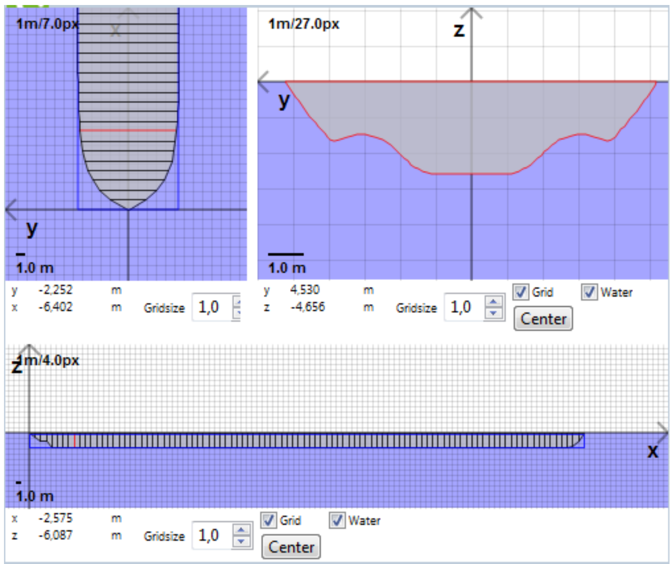

Figure 2: The tool HULK developed at the BAW to import ship models for FaRAO.

2.2 *Mathematical Model*

To describe the motion of the ship on the water surface a 3-DoF model is employed (Kolarov 2006). This model describes the longitudinal and transversal ship speeds $\vec{v} = (v_x, v_y)^T$ and the rotational speed ω in a flow field with spatially varying flow velocities $\vec{v}_{str} = (v_{flow,x}, v_{flow,y})^T$. The momentum conservation equations are given by

$$\frac{d}{dt}\left(mv_x + \int_L \bar{m}_x\, v_{a,x} d\xi\right) - \omega\left(mv_y + \int_L \bar{m}_y v_{a,y} d\xi\right) = X$$

$$\frac{d}{dt}\left(mv_y + \int_L \bar{m}_y\, v_{a,y} d\xi\right) - \omega\left(mv_x + \int_L \bar{m}_x v_{a,x} d\xi\right) = Y$$

$$\frac{d}{dt}\left(I_z\omega + \int_L \xi \bar{m}_y v_{a,x} d\xi\right) = N$$

with

m	mass [kg]
I_z	mass moment of inertia [kg m^2]
X, Y	external forces [N]
N	external moment [mN]
$\bar{m}_x, \bar{m}_y$	added mass per ship length [kg/m]
L	ship length [m]
ξ	local x-coordinate on ship [m]

and the local hydrodynamic velocities

$$v_{a,x} = \left(v_x - v_{flow,x}\right)$$
$$v_{a,y} = \left(v_y + \omega\xi - v_{flow,y}\right)$$

for $\xi \epsilon [0, L]$.

The added mass densities $\bar{m}_x$, $\bar{m}_y$ are functions of the local waterdepth h and are calculated during pre-processing based on potential theory. The ships hydrodynamic masses and moment are given by

$$m_x = \int_L \bar{m}_x d\xi,$$

$$m_y = \int_L \bar{m}_y d\xi,$$

$$I_{hz} = \int_L \xi^2 \bar{m}_x d\xi\ .$$

All entities so far are given in the ship coordinate system *0-x-y*; to track the global position in the 0_0-x_0-y_0 coordinate system (cf. Figure 3), the three additional ordinary differential

$$\dot{x} = v_x \sin\psi - v_x \cos\psi$$
$$\dot{y} = v_x \cos\psi + v_x \sin\psi$$
$$\dot{\psi} = \omega$$

equations have to be solved.

After some algebraic operations under careful consideration of the time depencies of the variables, the system can be formulated as ordinary differential equation (ODE)

$$\dot{\vec{x}} = f(\vec{x})$$

for the state function

$$\vec{x} = \left(v_x, v_y, \omega, x, y, \psi\right)^T$$
$$\vec{x}: [t_0, t_{end}] \to \mathbb{R}^6,$$

and the righthandside function

$$f = (f_1, f_2, f_3, f_4, f_5, f_6)^T$$
$$f: \mathbb{R}^6 \to \mathbb{R}^6$$

with

$$f_1 = M_x^{-1}\Big(X - \int_L \frac{d\bar{m}_x}{dt} v_{a,x} - \bar{m}_x \frac{dv_{str,x}}{dt} d\xi + \omega\left(m\, v_y + \int_L \bar{m}_y v_{a,y} d\xi\right)\Big)$$

$$f_2 = \left(M_y + \frac{S_y^2}{M_z}\right)^{-1}\Big(Y - \int_L \frac{d\bar{m}_y}{dt} v_{a,y} d\xi + \int_L \bar{m}_y \frac{dv_{str,y}}{dt} d\xi - \omega\left(m\, v_x + \int_L \bar{m}_x v_{a,x} d\xi\right) - \frac{S_y}{M_z}\Big(N - \int_L \xi \frac{d\bar{m}_y}{dt} v_{a,y} - \xi \bar{m}_y \frac{dv_{str,y}}{dt} d\xi\Big)\Big)$$

$$f_3 = \left(I_z + \frac{S_y^2}{M_y}\right)^{-1}\Big(N - \int_L \xi \frac{d\bar{m}_y}{dt} v_{a,y}\, d\xi + \int_L \bar{m}_y \frac{dv_{str,y}}{dt} d\xi - \frac{S_y}{M_y}\Big(Y - \int_L \frac{d\bar{m}_y}{dt} v_{a,y} d\xi + \int_L \bar{m}_y \frac{dv_{str,y}}{dt} d\xi - \omega\left(m\, v_x + \int_L \bar{m}_x v_{a,x} d\xi\right)\Big)\Big)$$

$$f_4 = v_x \sin\psi - v_x \cos\psi$$
$$f_5 = v_x \cos\psi + v_x \sin\psi$$
$$f_6 = \omega,$$

the effective masses

$$M_x = m + m_x$$
$$M_y = m + m_y,$$

the corresponding moment of inertia

$$M_z = I_z + I_{hz}$$

and the hydrodynamic mass center

$$S_y = \int_L \xi \bar{m}_y d\xi.$$

By formulating the dynamic system in terms of a general ordinary differential equation we can apply standard mathematical theory on existence and uniqueness of solutions.

As the dynamic system only models the inertia of the ship and the surrounding water, the hydrodynamic forces on the ship have to be considered as external forces.

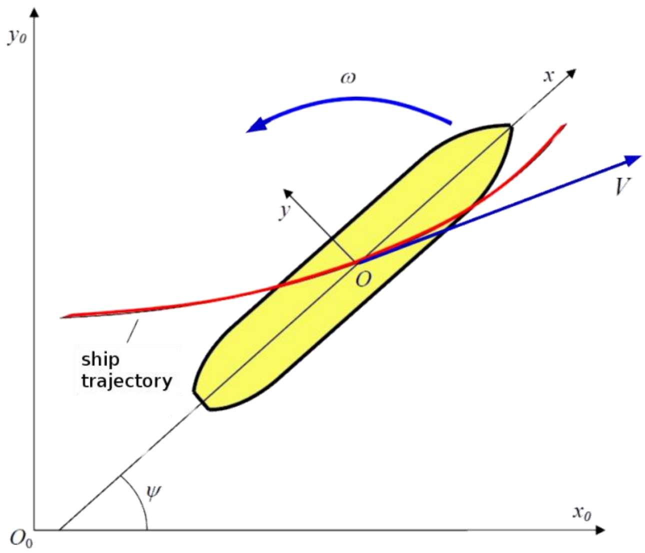

Figure 3: The coordinate systems for the dynamic system

2.3 External forces

The external forces acting on the ship are given by

$$X = X_{hl} + X_{cnt}$$
$$Y = Y_{hl} + Y_{cnt}$$
$$N = N_{hl} + N_{cnt}$$

with the hull forces X_{hl}, Y_{hl}, N_{hl} modelling the hydrodynamic forces on the underwater body of the vessel and the propulsion forces X_{cnt}, Y_{cnt}, N_{cnt} modelling the ship thrusters and steering devices, typically consisting of engine, rudder and bow thruster forces.

2.3.1 *Hull Forces*

For the hull forces, we consider three different components:

The ship resistance X_{res} is caused by friction, form of the hull and water level slope. We use a modified Graewe formula, which considers all three components. Details can be found in Wassermann et al. (2010).

The linear lateral force Y_{lin} and moment N_{lin} due to lift are calculated using the slender body approach based on the rate change of the fluid momentum along the length of the ship described by Toxopeus (2006).

The non-linear lateral force Y_{nl} and moment N_{nl} are caused by drag and are calculated with the method described by Hooft & Quadvlieg (1996).

The two latter forces and moments are adaptions of concepts for seagoing ships to varying water depth and flow velocities, while the first force was developed explicitly for inland vessels.

With these components the hull forces are given by

$$X_{hl} = X_{res}$$
$$Y_{hl} = Y_{lin} + Y_{nl}$$
$$N_{hl} = N_{lin} + N_{nl}.$$

Hull forces as those from ship-ship and ship-bank interactions are neglected at the present state of development and in current applications replaced by corresponding safety distances (VBW 2013).

2.3.2 *Propulsion forces*

The propulsion forces are given by

$$X_{cnt} = X_{prop}(n_{prop}) + X_{rud}(\delta_{rud})$$
$$Y_{cnt} = Y_{rud}(\delta_{rud}) + Y_{bsr}(f_{bsr})$$
$$N_{cnt} = N_{rud}(\delta_{rud}) + N_{bsr}(f_{bsr})$$

with the main engine force X_{prop} as function of the engine speed n_{prop}, the rudder forces X_{rud}, Y_{rud} and moment N_{rud} as functions of the rudder angle δ_{rud} and the bow thruster force Y_{bsr} and moment N_{bsr} depending on the frequency f_{bsr}. The specific models for the forces as well as their calibration for several common drive group setups are subject research projects within the BAW.

2.4 *Summary*

By assembling the controls for rudder, propulsion and bow thruster in the control function

$$\vec{u} = (n_{prop}, \delta_{rud}, f_{bsr}): [t_0, t_{end}] \to \mathbb{R}^3$$

the ODE can be reformulated as the control-dependent initial value problem

$$\dot{\vec{x}} = f(\vec{x}, \vec{u})$$
$$\vec{x}(t_0) = \vec{x}_0.$$

With an startpoint $\vec{x}_0$, this formulation allows the use of standard numerical integration methods for the solution of the initial value problem. By solving the initial value problem one yields exactly one state function $\vec{x}$ for a given control function $\vec{u}$. With this state function further evaluations such as the occupied space (swept path) in the waterway or the course deviation from the desired path can easily be calculated.

3 COURSE FOLLOWING ALGORITHM

To examine a given ship trajectory - for example from field measurements or simulator runs – it is necessary to have a procedure to find controls $\vec{u}$ so the ship in the fast-time simulator follows the given trajectory. With these controls it is possible to evaluate e.g. the swept path or the forces acting on the ship sailing along the given trajectory.

We suggest an optimal control approach that is based on the idea that a pilot is able to look a certain time t_{fore} ahead. During this foresight time he/she sets the control $\vec{u}$ to stay as close to the given path as possible. The corresponding optimal control problem (OCP) is given by

$$\min_{\vec{x},\vec{u}} J(\vec{x},\vec{u}) = \int_{t_0}^{t_0+t_{fore}} (\vec{x}^* - \vec{x}^*)^2 dt$$

$$s.t.\ \vec{x}(t) = \vec{x}_0 + \int_{t_0}^{t} f(\vec{x},\vec{u}) dt.$$

As this approach tends to underestimate the effect of the rudder angles in the vicinity of t_{fore}, the solution is only accepted up to a trust time t_{trust}. After this threshold is reached, a new optimal control problem has to be considered. The procedure is given in Algorithm 1. The optimal control problem is solved by a gradient method in a 'first-discretize-then-optimize' approach. The necessary first order derivatives are obtained by finite differences.

One advantage of this optimal control approach is the possibility to adapt the functional $J(\vec{x},\vec{u})$ to solve for other criteria such as energy or time optimal trajectories. Of course other approaches such as a feedback control will be considered at a later point of time.

By using a model for the pilot, it is possible to alter the parameters such as the foresight time t_{fore} to model the influence of individual control behaviour and to investigate the impact of the human factor on safe and swift maneuvering. In future development it will be considered to implement pilots with individual response times and error susceptibilities.

```
pilot-> getControl(time):
      if time>t_trust
           setup OCP
           solve OCP with gradient method
           store results in table
      return u⃗(time) from table
```

Algorithm 1: Procedure for the course following pilot.

4 SOFTWARE FRAMEWORK

FaRAO is the successor of PeTra2D (German: Pegelabhängige Trassierung) developed by Kolarov (2006). Major objectives of the reengineering were the ease of future enhancements such as the optimization of ship paths according to different optimization aims, the simulation of ship induced waves and currents, the implementation of an autopilot modelling human

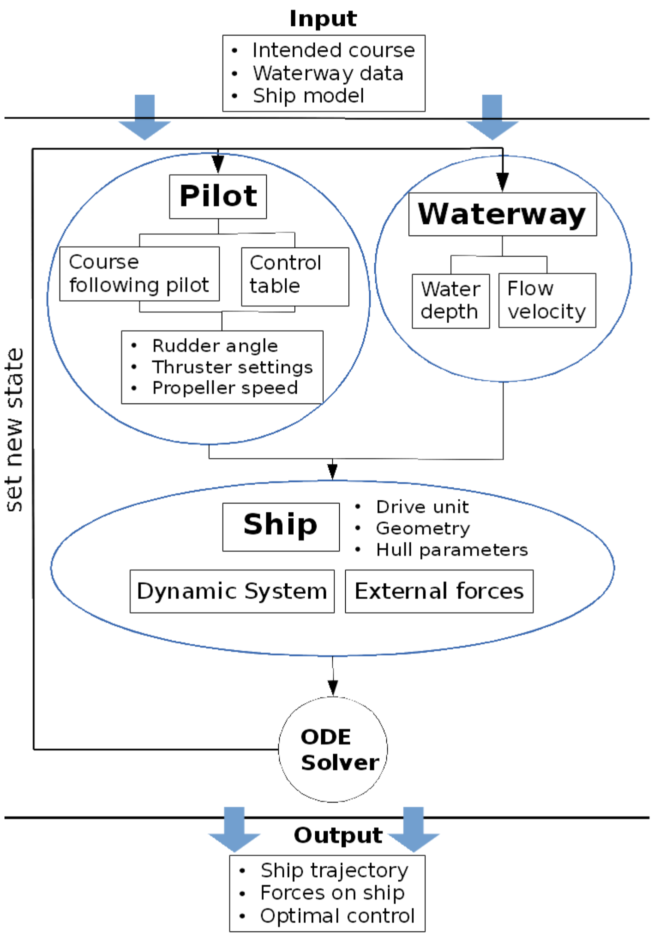

Figure 4: Simulation work flow of FaRAO

properties to examine the impact of human behavior on necessary navigational space and bank protection as well as the ability to run the software HPCs. The new software is based on modular design and implemented in C++.

The upper level modules are

- *Ship*: computes all elements of the dynamic system and the external forces
- *Waterway:* spatial distribution of flow velocities and water depth
- *Pilot:* controls rudder, engine and bow thruster; has therefore access to optimization algorithms and the objective function

The workflow is shown in Figure 4. The modular design enables e.g. the activation and deactivation of additional force terms or the replacement of a drive group by another one with minimal effort.

5 NUMERICAL TESTS

In this section we will show a convergence analysis for the given dynamic system as well as two numerical examples testing the course following pilot. All computations were carried out on a desktop computer with 8GB RAM and an Intel Core i5-4570 in a single thread.

5.1 Convergence analysis

For this test case we consider a ship driving into a cross flow field for a simulation time of $t_{sim} = 400\,s$ without altering the rudder angle. The trajectory of the ship is calculated using the explicit Euler method for the numerical step sizes Δt ={1.0 s, 0.5 s, 0.25 s, 0.125 s, 0.0625 s}. As no analytical solution is available, we compare the resulting trajectories with a higher order solution $\vec{x}_{ref}$. We use a 4th order Runge-Kutta method with a numerical step size of Δt =0.01 s to obtain this reference solution. The mean deviation is given by

$$\bar{\epsilon} = \frac{\left(\int_{t_0}^{t_{end}} (\vec{x}_{ref} - \vec{x})^2 dt\right)^{1/2}}{t_{end} - t_0}.$$

As expected, the mean deviation is increasing with the step size Δt (cf. Table 1), with the only exception at $\Delta t = 1.0\,s$. By analyzing the course deviation over time we see that $\Delta t = 1.0\,s$ behaves substantially different than the smaller step sizes (cf. Figure 5). As result it seems reasonable to exclude numerical step sizes larger than 0.5 s. By taking a look at the computational time, we see the expected linear dependency between the computational time t_{cpu} and the numerical step size Δt. Even for the smallest considered numerical step size, a speedup $t_{sim}/t_{cpu} > 250$ is reached.

Table 1: Error analysis for the solution of a simulation with $t_{sim} = 400\ s$

numerical step size Δt	mean deviation $\bar{\epsilon}$	computational time t_{cpu}
1.0	0,0320	0,09 s
0.5	0,0375	0,19 s
0.25	0,0218	0,37 s
0.125	0,0072	0,73 s
0.06125	0,0019	1,52 s

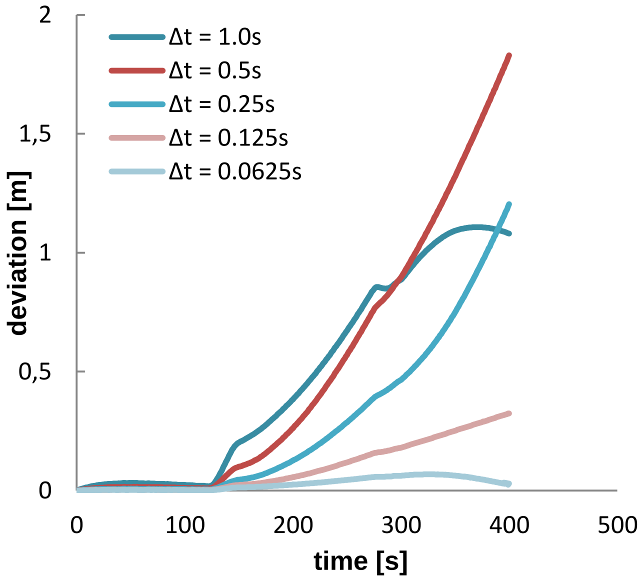

Figure 5: Error analysis for different numerical step sizes.

5.2 *Lateral offset maneuver*

In this maneuver the ship starts with a lateral offset from the desired course of 2 m and a forward velocity of 3.5 m/s. As the rudder angle is the only control parameter, the ship has to perform two turns to get back on the course.

The rudder angles are calculated by the course following pilot introduced in section 3 with $t_{fore} =$ 100 s and $t_{trust} =$ 10 s. The resulting course deviation, rudder and drift angle are shown in Figure 6. The maneuver is completed after about 100 s. The large number of objective function evaluations (9 264, cf. Table 2) caused by the finite differences of the gradient method explains the computational time of $t_{cpu} =$ 680.3 s which is well above real time. Each objective function evaluation equals a simulation run with $t_{sim} =$ 100 s. By further investigation of the optimization procedure it should be possible to accelerate the computations beyond real time.

5.3 *Passing a cross flow field*

In this test case the ship passes a cross flow of a limited width of 500m while the course following pilot tries to keep a course steady ahead. The resulting maximum deviation from the set course is below 1 m. After the ship has entered the cross flow it takes a constant drift angle of 8.54 ° and sets the rudder angle to 0° until it reaches the end of the cross flow (cf. Figure 7).

As this problem can be solved with a smaller foresight time t_{fore}= 50 s, we yield a computational time smaller then simulation time despite the large number of objective function evaluations (18 935, cf. Table 2).

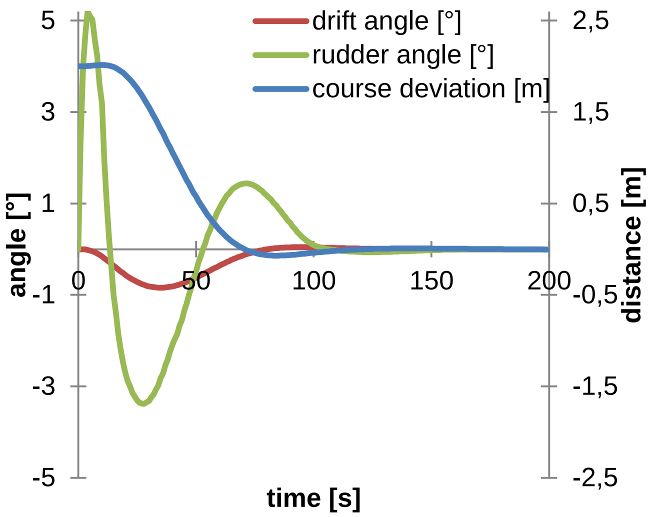

Figure 6: Ship performing a lateral offset maneuver controlled by the course following pilot

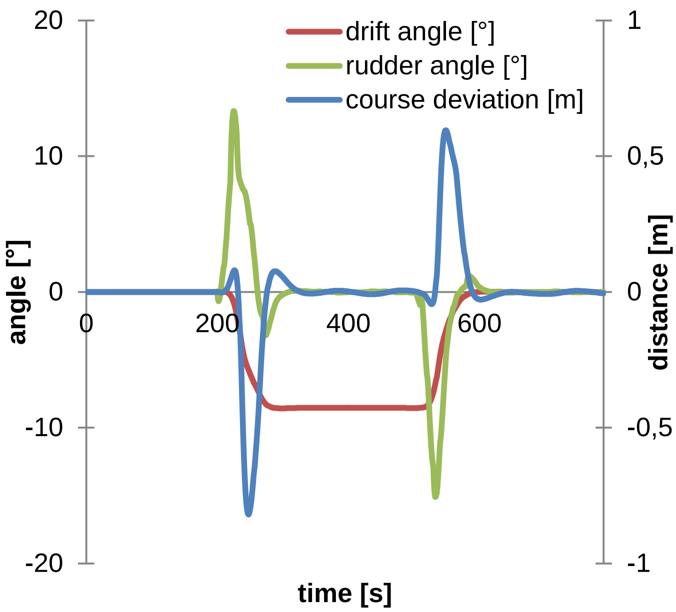

Figure 7: Ship sailing through cross flow field controlled by the course following pilot.

Table 2: Numerical parameters and results for the lateral offset maneuver and the cross flow passing

	lateral offset maneuver	passing of a cross flow
simulation time t_{sim}	200.0 s	800.0 s
comp. time t_{cpu}	680.3 s	694.9 s
foresight time t_{fore}	100.0 s	50.0 s
#obj. function eval.	9 264	18 935

6 CONCLUSION

The fast-time simulator FaRAO allows calculation of trajectories for ships based on geometric properties and a very limited number of calibration parameters. As computational times are several hundred times shorter then simulation times it is possible to use numerical optimization algorithms for following a given course in close-to real-time. Further investigations of the optimization algorithm as well as performance analysis should allow the application of these procedures in real time. This makes the fast-time simulator FaRAO a promising tool for carrying out comparative variant analysis in an effective manner as the vessels can be repeatedly steered in the exact same manner (Söhngen & Eloot 2014). The enhancement of the optimization towards automatic determination of optimal trajectories with respect to fuel consumption, travel time and navigational space will be subject to further research.

Not yet considered are forces due to ship-bank and ship-ship interaction and wind forces. These are subject of ongoing research. While the estimation of these forces might be difficult, their implementation is not as the chosen modular design allows for an easy enhancement of additional force terms.

7 Acknowledgement

This study was carried out as part of ongoing projects optimizing the transport infrastructure of the German rivers Necker and Danube by the Bundesanstalt für Wasserbau (BAW).

REFERENCES

Toxopeus, S.L. 2006, Validation of slender-body method for prediction of linear manoeuvring coefficients using experiments and viscous flow calculations, *ICHD2006: 7th International Conference on Hydrodynamics*

Hooft, J.P. and Quadvlieg, F.H.H.A. 1996, Non-linear hydrodynamic hull forces derived from segmented model tests. *MARSIM International Conference on Marine Simulation and Ship Manoeuvribility*

Kolarov, P. 2006, Simulation von Schiffs-bewegungen in Fließgewässern, *Diss., Universität Rostock.*

Söhngen, B. 2015, Application of WG 141 approach including elaboration of field data and fast time simulation for Class Va-vessel passing narrow Jagstfeld bridge in the German Neckar River. *PIANC Smart Rivers 2015.*

Söhngen, B and Eloot, K. 2014, Update PIANC INCOM WG 141: Design guidelines for inland waterways. 33rd *PIANC World Congress.*

VBW 2013, Fahrdynamik von Binnenschiffen, *Fachausschuss Binnenwasserstraßen und Häfen (VBW/HTG) und Fachausschuss für Binnenschiffe (VBW/STG), Germany.*

Wassermann, S., Söhngen, B., Dettmann, T. and Heinzelmann, C. 2010, Investigations to define minimum fairway widths for inland navigation channels. *32nd PIANC World Congress.*